Plasmonic metaresonances: Molecular resonances in quantum dot–metallic nanoparticle conjugates

S. M. Sadeghi*
Department of Physics, University of Alabama in Huntsville, Huntsville, Alabama 35899, USA
(Received 14 May 2009; revised manuscript received 8 June 2009; published 26 June 2009)

The basic excitations of noble metallic nanoparticles and semiconductor quantum dots are, respectively, surface plasmons and excitons. In this Brief Report it is shown that when these nanostructures are conjugated together, their combined hybrid system can support a meta- "molecular" resonance. Such a resonance happens in the space/time domain and is associated with the time delay induced by the plasmonic effects in the response of the quantum dot to a time-dependent optical field. The metaresonance happens when the distance between the quantum dot and the metallic nanoparticle reaches a critical value and the time delay goes to infinity. The results demonstrate generation of Rabi oscillation in quantum dots via plasmons and offer alternative ultrasensitive methods for sensing.

DOI: 10.1103/PhysRevB.79.233309 PACS number(s): 73.21.La, 71.35.Cc

Optical properties of noble-metal nanoparticles (MNP) are mostly associated with their localized surface-plasmon resonances. When a MNP is excited by an electromagnetic radiation field, at such a resonance it exhibits collective oscillations of its conduction electrons. Surface plasmons in MNPs are desirable for many technological applications. For example, it has recently been demonstrated that coupling of such plasmons in linear chains of MNPs results in transport of light along the chains.[1–3] Plasmonic resonances are also quite useful for many other applications including sensors,[4,5] nanoscale optical devices, imaging, etc.[6] Conjugates of MNPs with semiconductor quantum dots (QDs) have also been studied extensively.[7,8] It has been shown that in such nanoparticle molecules one can modify energy transfer between quantum dots,[9] enhance or suppress their emission,[10–13] modify heat dissipation in MNPs, etc.[7,8]

One of the objectives of this Brief Report is to show, similar to diatomic molecules, when QDs and MNPs with primary exciton and plasmon excitations are conjugated together, their combined systems can support a meta- "molecular" resonance, called here plasmonic metaresonance (PMR). This resonance is associated with the time delay (τ_p) induced in the response of a QD to a time-dependent optical field when it is at the vicinity of a MNP. During this period of time, because of the strong exciton-plasmon coupling, population density and polarization of excitons are governed by dynamic normalization of their energies and linewidths, and by significant screening and reshaping of applied optical field via plasmonic effects. PMR occurs when τ_p goes to infinity abruptly. When refractive index of the host medium is considered constant, PMR happens when the distance between the QD and MNP reaches a critical value (R_c). We discuss the origins of the plasmonic time delay and PMR in detail and investigate how R_c depends on the applied optical-field intensity and time dependency. PMR offers a new class of ultrasensitive sensing techniques, including detection of distance up to subnanometer resolution using conventional optical techniques.

Another objective of this Brief Report is to demonstrate how plasmonic effects can dramatically modify the optical field experienced by a QD. The effective field not only can be different from the external field in terms of its amplitude, but also in terms of its time dependency. As a result, in addition to significant screening during τ_p, the rise time of the effective field can be significantly shorter than that of the applied field. Therefore, as shown in this Brief Report, when the external optical field cannot generate Rabi flopping because of its slow rise, significant Rabi oscillation can be induced when the QD is close to the MNP. This effect and formation of complex Rabi frequency illustrated in the following suggest quantum optics of QDs in the presence of plasmonic effects can be distinctively different from that of isolated QDs. Note that recently we studied a similar hybrid system embedded in an environment with rather low permittivity.[14] Several key issues were identified, including slight amount of plasmonic time delay and enhancement of Rabi flopping. PMR, however, did not happen in such a system, since its formation required unrealistic proximity between the QD and MNP. Additionally, because of the low permittivity of the environment, plasmonic effects in this system did not generate Rabi oscillation, rather only enhanced it.

Our prime interest in this Brief Report is to study dynamic response of a QD when it is interacting with a time-dependent optical field ($E_{\text{app}}(t)=\frac{1}{2}E_0^{\text{app}}(t)e^{-i\omega t}$). For this we consider the QD is conjugated with an Au MNP with radius $a=7$ nm, forming a hybrid system. The matrix holding this system is considered to have dielectric constant ε_0. The center-to-center distance between the nanoparticles is denoted as R. The interaction between the QD and the MNP is characterized by the large electric-dipole moments of the QD and plasmon resonance of the MNP. We consider the electric field is polarized along the z direction joining the two particles. The MNP has nanoscale dimension and, therefore, its interaction with the laser field is treated within quasistatic approximation. We describe the MNP with the local dynamic dielectric function ε_m. The applied optical field (E_{app}) is considered to have a steplike rise time with final intensity I. The frequency of this laser (ω) is considered to be the same as that of the transition between the ground and the first exciton state of the QD (the 1–2 transition) when its coupling to the MNP is insignificant (large R). We also consider the frequency of the MNP plasmon resonance is the same as that of the 1–2 transition.

Under these conditions we obtained equation of motion for the density matrix of the QD coupled to the MNP as follows:[14]

$$\frac{\partial \rho_{11}}{\partial t} = -2\,\mathrm{Im}[\Omega_{12}^{r}\rho_{21}] + \Gamma_{22}\rho_{22} - \Gamma_{11}\rho_{11}, \tag{1}$$

$$\frac{\partial \rho_{22}}{\partial t} = +2\,\mathrm{Im}[\Omega_{12}^{r}\rho_{21}] - \Gamma_{22}\rho_{22}, \tag{2}$$

$$\frac{\partial \rho_{21}}{\partial t} = -[i\Delta_{12} + \gamma_{21}]\rho_{21} - i\Omega_{12}^{r}(\rho_{11} - \rho_{22}). \tag{3}$$

Here $\Delta_{12}=\omega_{21}-\omega$ where ω_{21} is the frequency associated with the 1–2 transition. $\Omega_{12}^{r}=\Omega_{12}^{\mathrm{eff}}-\eta\rho_{21}$ is the normalized Rabi frequency with $\Omega_{12}^{\mathrm{eff}}=\Omega_{0}^{12}(1+\frac{2\gamma a^3}{R^3})$. $\Omega_{12}^{0}=-\frac{\mu_{12}E_0^{\mathrm{app}}}{2\hbar\varepsilon_{\mathrm{eff1}}}$ is the Rabi frequency when the QD is isolated (very large R) and $\gamma=\frac{\varepsilon_m(\omega)-\varepsilon_0}{\varepsilon_m(\omega)+2\varepsilon_0}$. $\eta=\eta_r+i\eta_{\mathrm{im}}$ is given by

$$\eta = \frac{4\gamma\mu_{12}^2}{\hbar\varepsilon_{\mathrm{eff1}}^2}\frac{a^3}{R^6}. \tag{4}$$

Γ_{ij} and γ_{ij} introduced above refer to energy and polarization relaxation rates of the isolated QD, respectively. We consider $\Gamma_{22}=1/0.8$ ns^{-1} and $\mu_{12}=0.65e\times$nm.[7] The dephasing broadening of the single QD is considered 2.7 ns^{-1}.[7,8] Note that Eqs. (1)–(3) represent optical Bloch equations wherein the plasmonic and optical effects are all embedded into the normalized Rabi frequency. Optical Bloch equations have also been used to study molecular excitation near a MNP chain,[3] or study radiative and nonradiative decay channels experienced by a single molecule confined in an adjustable dielectric-metal nanogap.[15] Enhancement of emission of QDs or molecules has also been studied using rate equations.[12,13]

We consider $\varepsilon_0=1.8$, corresponding to host materials such as water. For such a matrix the plasmon peak occurs at about 2.37 eV. To study the impact of the plasmonic effects on the interaction of the QD with the optical field, first it is constructive to consider how Ω_{12}^{r} is changing with R and time. This quantity shows how such interaction is normalized by the NMP. As shown in Fig. 1(a), for $R=100$ nm (line 1) the real part of Ω_{12}^{r} in fact represents variation in the applied optical field with time. This is because of the fact that under this condition the plasmonic effects are insignificant and $\Omega_{12}^{r}=\Omega_{12}^{0}$. For smaller R's, however, variation of Ω_{12}^{r} with time varies dramatically from that of $R=100$ nm (lines 2 and 3). Two significant effects here include time delay (τ_p) in the rise of $\mathrm{Re}[\Omega_{12}^{r}]$ compare to that of the optical field (line 1) and generation of some oscillatory features. The latter is because of the fact that, as seen above, through plasmonic effects normalized Rabi depends on the off-diagonal elements of the density matrix.

As the QD gets closer to the MNP the amount of the time delay increases super linearly. As shown in Fig. 1(b), sensitivity of τ_p to R can be so significant that for just 0.01 nm change in R, i.e., from 15.48 (line 5) to 15.47 nm (line 6), τ_p can be increased by about 40 ns. Another significant feature is that for any value of R within τ_p the magnitude of real part

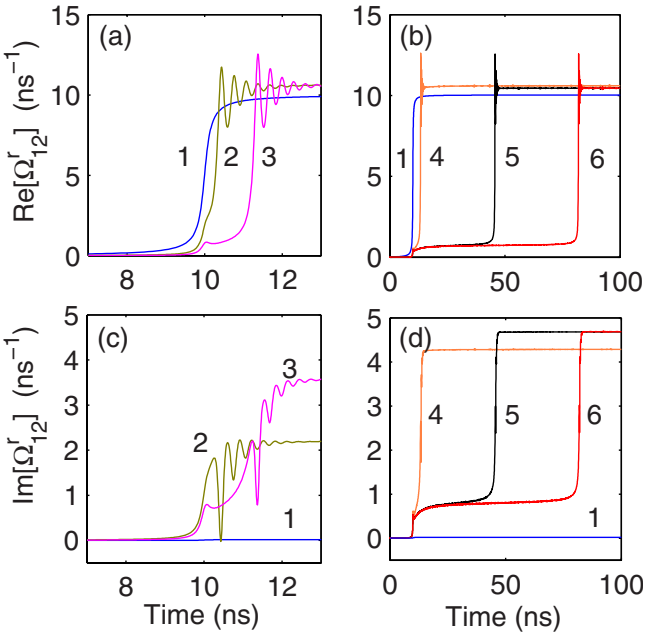

FIG. 1. (Color online) Variation in real [(a) and (b)] and imaginary [(c) and (d)] parts of normalized Rabi frequency with time for $I=128$ W/cm^2 and different R's. Lines 1, 2, 3, 4, 5, and 6 refer, respectively, to $R=100$, 20, 17, 16, 15.48, and 15.47 nm.

of Ω_{12}^{r} is relatively quite small. It is, however, increasing monotonously at low rate. Additionally, the small rise of $\mathrm{Re}[\Omega_{12}^{r}]$, which happens at the same time as the full rise of the applied optical field (line 1), does not cause any significant oscillation. The second rise, however, that occurs after τ_p comes with significant overshoots and oscillations. These results show that the field experienced by the QD in the presence of the MNP can be significantly different from that of the applied field. Even after τ_p and reaching steady state the values of $\mathrm{Re}[\Omega_{12}^{r}]$ for small R are more than Ω_{12}^{0}, suggesting enhancement of optical excitation, as will be discussed in the following. Additionally, Fig. 1 suggests that normalized Rabi frequency is a complex quantity. Figures 1(c) and 1(d) show the corresponding variations of $\mathrm{Im}[\Omega_{12}^{r}]$ with R and time.

Under the same conditions as those of Fig. 1 the corresponding evolutions of exciton population with respect to time are shown in Figs. 2(a) and 2(b). These results are consistent with the results obtained for normalized Rabi frequency in Fig. 1. For $R=100$ nm Fig. 2(a) shows a standard Rabi flopping (line 1).[16] For smaller R the amplitudes of the overshoots are decreased as ρ_{22} reaches its final value with some time delay. Figure 2(b) shows that for R around 15 nm (lines 4 and 5), we see significant amount of delay in the population excitation and formation of saturation. Note that, similar to Ω_{12}^{r}, ρ_{22} initially increases from zero without any overshoot. Then it increases monotonously at a low rate and finally ramps up sharply, causing some Rabi flopping.

The prime effects seen above included formation of τ_p and its super linear increase with the decrease of R. This process has a limit beyond which τ_p becomes infinite, i.e., PMR occurs. Figure 3 illustrates formation of PMR for two different I's. When $I=32$ W/cm^2, R_c is about 18.01 nm

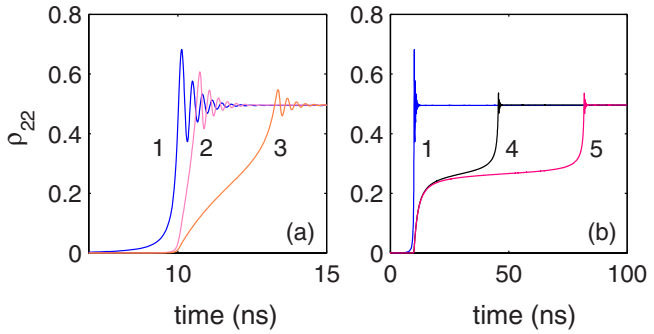

FIG. 2. (Color online) Variation of ρ_{22} with time for various values of R when $I=128$ W/cm^2. Lines 1, 2, 3, 4, and 5, refer, respectively, to $R=100$, 18, 16, 15.5, and 15.47 nm.

(dashed line), while for $I=128$ W/cm^2 R_c is reduced to 15.46 nm (solid line). For I's smaller than 32 W/cm^2 formation of PMR is smeared out. In fact for I around 5 W/cm^2 this effect does not happen. Note that for any value of R smaller than R_c, τ_p remains always infinite.

The PMRs seen in Fig. 3 temporally separate two different types of mechanisms that govern dynamics of excitons in a QD when it is in the vicinity of a MNP. The results suggest that after the plasmonic time delay, the system behaves somehow similar to an isolated QD. Here, however, the impacts of plasmons are translated into normalized Rabi frequency obtained under steady state. Figure 1 shows that $\Omega_{12}^r > \Omega_{12}^0$, suggesting that in a QD-MNP hybrid system plasmonic effects can enhance exciton excitation rate in the QD. Such a process was not observable in Figs. 2(a) and 2(b), since we considered the optical-field resonant with the 1–2 transition of the QD and, therefore, saturation prevents this effect to show up. If one considers an off-resonance case, wherein saturation does not happen, such an enhancement process can become quite visible.

To study the physics behind plasmonic time delay and PMR, let's reconsider Eq. (3) and rewrite it in a more explicit form

$$\frac{\partial \rho_{21}}{\partial t} = -[i(\Pi_{12} - \omega) + \Lambda_{21}]\rho_{21} - i\Omega_{12}^{\text{eff}}(\rho_{11} - \rho_{22}). \quad (5)$$

In this equation $\Pi_{12}=\omega_{21}-\eta_r(\rho_{11}-\rho_{22})$ is the normalized energy of the exciton transition and $\Lambda_{21}=\gamma_{21}+\eta_{\text{im}}(\rho_{11}-\rho_{22})$ is

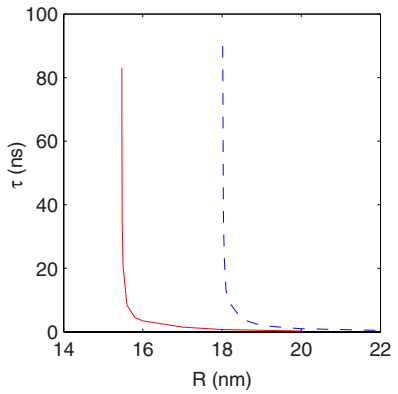

FIG. 3. (Color online) Variation of the τ_p with R for $I=128$ (solid line) and 32 (dashed line) W/cm^2.

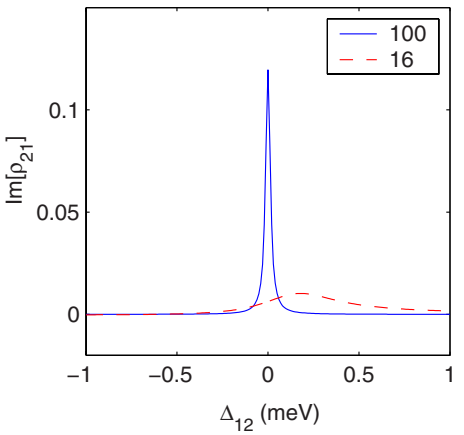

FIG. 4. (Color online) Imaginary part of ρ_{21} for $R=100$ (solid line) and 16 (dashed line) nm. The intensity of the probe field is assumed to be 0.3 W/cm^2.

Forster-enhanced broadening of this transition. These parameters quantitatively describe how the transition energy and lineshape of the QD are changed as it becomes close to the MNP. They depend not only on η, but also on the exciton population density, optical-field intensity, and time. When the optical field is weak their impacts can be significant. Therefore, before the applied optical field arrives or its rise happens, the QD transition and broadening, depending on the values of R, can be extensively normalized by plasmonic effects. This is illustrated in Fig. 4, where we show a steady-state solution for Im$[\rho_{21}]$ considering the intensity of the probe field (applied optical field) is 0.3 W/cm^2.

Figure 5(a) shows dynamic detuning of the optical field from the normalized interband transition of the QD for different R. As in Figs. 1–3, we consider this field is resonant with the 1–2 transition when R is very large. The results show that, when $R=100$ nm the optical field remains resonant with this transition at all times (solid line). But for smaller R three main features can be seen: (i) before the applied optical-field rise the photon energy of this field is larger than that of the 1–2 transition of the QD, (ii) during τ_p the energy of the QD transition is dynamically increased, (iii) after τ_p the optical field becomes resonant with the 1–2 transition. For $R=20$ nm (dashed line), however, the amount of the red shift in this transition is relatively small. Therefore, the system does not show significant delay and quickly goes into the state where $\Pi_{12}=\omega_{12}$ and $\Lambda_{12}=\gamma_{12}$. For smaller R the initial shift is significant. Therefore, the optical field is at the beginning quite off-resonant from the normalized QD transition. Therefore, optical excitation is hindered significantly. This picture becomes clearer considering how the damping of the QD transition changes with R and time [Fig. 5(b)]. It is evident here that as R decreases this transition becomes more broadened, resisting optical excitation. These effects are in accordance, in particular, with the results in Fig. 1 wherein we showed plasmonic screening of the applied optical field. The plasmonic time delay is formed due to the interplay between these dynamic effects that hinder full excitation of the system for a period of time. PMR, on the other hand, happens when the rate of increase in normalized Rabi frequency during the delay goes to zero, making the time delay infinite.

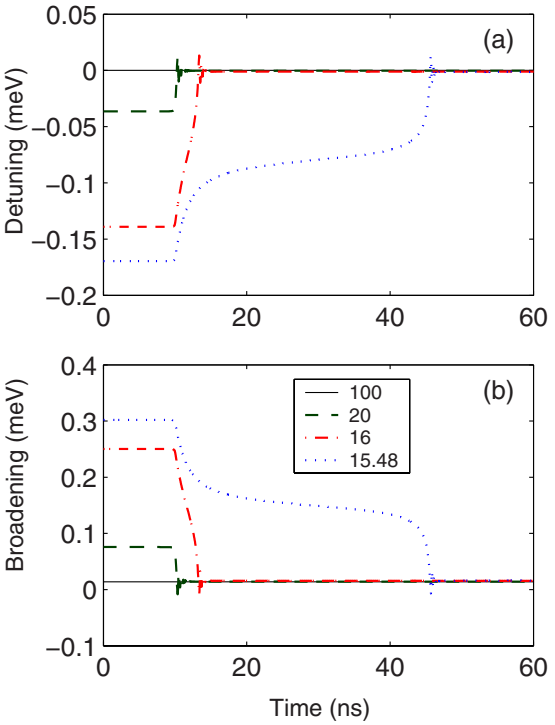

FIG. 5. (Color online) Dynamic variation in the optical field detuning from the QD transition (a) and broadening of this transition (b) for different R's as a function of time. The legends show R's in nm.

Note that the effects discussed in this Brief Report remain significant even when the rise time of optical field is quite long. Figure 6 shows the case when the rise time happens over about 50 ns. Several interesting effects are evident here: (i) although the rise time of the applied optical field is long (line 1), as shown in (a) and (b), the field experienced by the QD after τ_p can have much shorter rise times, (ii) because of this while the external optical field is too slow to induce Rabi flopping, one expects to see Rabi flopping when R is small [Figs. 5(c) and 5(d)], and (iii) when time rise of the optical field is long, as seen in (b), the amount of delay can even reach 0.5 μs. Figure 6(d) clearly shows how plasmonic effect can induce Rabi flopping.

In conclusion, we showed that interaction of a QD with a

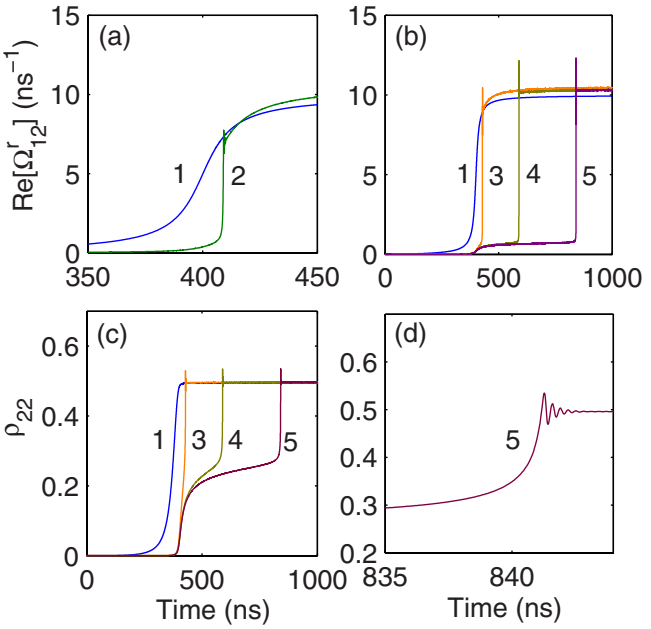

FIG. 6. (Color online) Variation in the normalized Rabi frequency [(a) and (b)] and ρ_{22} [(c) and (d)] for an applied optical field with much longer time rise. Here lines 1, 2, 3, 4, and 5 correspond to, respectively, R=100, 17, 16, 15.55, and 15.51 nm. Here I =128 W/cm^2.

time-dependent optical field in the presence of a MNP could lead to a two-stage coupling process. At the first stage the optical field is screened significantly by plasmonic effects, suppressing the field experienced by the QD dramatically. At the second stage the QD is driven by the optical field as if it is isolated but driven with a Rabi frequency normalized by the plasmonic effects. We demonstrated that the first stage corresponds to a plasmonically induced time delay in the response of the QD when it interacts with a time-dependent optical field. We also showed that when the distance between the QD and the MNP reaches a critical value, the delay becomes infinite. Under this condition the system always remains at the first stage. This suggests that, in addition to the primary plasmonic and exciton excitations, hybrids consisting QDs, and MNPs can support a secondary resonance, called here plasmonic metaresonance, due to the strong coupling between these two excitations.

*seyed.sadeghi@uah.edu

[1] M. Quinten, A. Leitner, J. R. Krenn, and F. R. Aussenegg, Opt. Lett. **23**, 1331 (1998).
[2] J. R. Krenn *et al.*, Phys. Rev. Lett. **82**, 2590 (1999).
[3] G. Colas des Francs, C. Girard, T. Laroche, G. Leveque, and O. J. F. Martin, J. Chem. Phys. **127**, 034701 (2007).
[4] A. Dahlin *et al.*, J. Am. Chem. Soc. **127**, 5043 (2005).
[5] A. J. Haes, L. Chang, W. L. Klein, and R. P. V. Duyne, J. Am. Chem. Soc. **127**, 2264 (2005).
[6] H. Imahori and S. Fukuzumi, Adv. Mater. **13**, 1197 (2001).
[7] W. Zhang, A. O. Govorov, and G. W. Bryant, Phys. Rev. Lett. **97**, 146804 (2006).
[8] R. D. Artuso and G. W. Bryant, Nano Lett. **8**, 2106 (2008).
[9] A. O. Govorov, J. Lee, and N. A. Kotov, Phys. Rev. B **76**, 125308 (2007).
[10] A. O. Govorov *et al.*, Nano Lett. **6**, 984 (2006).
[11] B. N. J. Persson and N. D. Lang, Phys. Rev. B **26**, 5409 (1982).
[12] G. Sun, J. B. Khurgin, and R. A. Soref, Appl. Phys. Lett. **94**, 101103 (2009).
[13] J. B. Khurgin, G. Sun, and R. A. Soref, Appl. Phys. Lett. **94**, 071103 (2009).
[14] S. M. Sadeghi, Nanotechnology **20**, 225401 (2009).
[15] G. Baffou *et al.*, Phys. Rev. B **77**, 121101(R) (2008).
[16] T. H. Stievater *et al.*, Phys. Rev. Lett. **87**, 133603 (2001).